International Journal of Coal Science & Technology (2024) 11:55
https://doi.org/10.1007/s40789-024-00713-w

RESEARCH

Moisture penetration and distribution characterization of hard coal: a μ-CT study

Lihai Tan[1] · Ting Ren[2,3] · Linming Dou[3] · Jian Sun[4] · Xiaohan Yang[4,5] · Ming Qiao[2]

Received: 20 June 2023 / Revised: 18 October 2023 / Accepted: 30 May 2024

Abstract
Moisture content of rock/coal can change its mechanical properties and absorption capacities, which can directly affect gas diffusivity, change the stress distribution and hence cause significant impacts on the overall gas or coal extraction process. Observation of the water penetration process and water distribution in the coal matrix will be beneficial for the understanding of the fluid-solid coupling mechanism in hydraulic fracturing, aquifer cracking and coal seam infusion. However, the observation of water penetration process and the determination of water distribution mode were hard to be non-destructively achieved as coal is a non-uniform, inhomogeneous and un-transparent material. μ-CT imaging, which is based on variation of X-ray attenuation related to the density and atomic composition of the scanned objects, enables a four-dimensional (spatial-temporal) visualise of the heterogeneous and anisotropic coal samples. The primary aim of this paper is extending the application of μ-CT imaging to explore the moisture penetration and distribution within coal samples during water infusion process, which has been reported by very little literature. The working principle and procedures of CT imaging was firstly introduced. Then, the determination equation of moisture distribution based on density profile was established. The CT determined moisture content has been compared with weighting method for verification. The paper has demonstrated that μ-CT can be used for non-destructively imaging the moisture distribution within coal samples.

Keywords Coal · Moisture distribution · μ-CT · Water saturation

1 Introduction

Moisture content of coal can affect the mechanical properties (Yao et al. 2019) and absorption capacities (Perera et al. 2011) of coal matrix, which can directly affect gas diffusivity, change the stress distribution and hence cause significant impact on the overall gas or coal recovery process (Liu et al. 2023). On one hand, moisture penetrating into the cleat system (Pan et al. 2010) due to natural aquifer or artificial hydro-fracturing can affect the gas effective permeability and overall gas diffusion behaviour. Hence, it is well recognised that coal matrix moisture can reduce the gas adsorption capacity and gas drainage productivity. On the other hand, the moisture softening, and pore pressure caused by moisture can affect the properties and the stress distribution within coal matrix (Ma et al. 2022), which will also indirectly have effect on the fracture propagation within coal (Liu et al. 2022). Observation of the water penetration process and water distribution in the coal matrix will be beneficial for the understanding of the fluid-solid coupling mechanism in hydraulic fracturing, aquifer cracking and coal seam infusion, hence, to contribute to the safety and cost-effectiveness of mining and resources industry. Previous studies focus more on the water effect on the absorption capacity and mechanical properties of coal (Du et al. 2019; Liu et al. 2021; McCarter 2010). However, the observation of water penetration process and the determination of

✉ Xiaohan Yang
yangxiaohan1994@gmail.com

1 School of Resource Environment and Safety Engineering, University of South China, Hengyang 412001, PR China

2 School of Civil, Mining and Environmental Engineering, University of Wollongong, Sydney, NSW 2522, Australia

3 State Key Laboratory of Coal Resources and Safe Mining, China University of Mining and Technology, Jiangsu 221116, PR China

4 School of Energy and Safety Engineering, Anhui University of Science and Technology, Anhui 232001, PR China

5 School of Civil Engineering, The University of Queensland, Brisbane, QLD 4072, Australia

Published online: 07 July 2024

water distribution mode were hard to be non-destructively achieved as coal is a non-uniform, inhomogeneous and untransparent material.

Generally, the moisture content of coal/rock is determined by calculating the weight losses before and after repeated oven drying till the weight change is below the targeted percentage of the sample weight (Australian Standard 2005). However, the water distribution can be significantly different between the water saturation and drying process even with the same moisture content measured by oven drying method. Moisture will concentrate on the surface area of the sample for the water saturation distribution, while the moisture on the surface will be firstly evaporated for the water drying distribution. Due to the undeveloped pore structure of hard coal (Li et al. 2023; Li, Ren, Li et al. 2023a, b), the sample needs several days to reach the uniform water distribution (fully saturated or totally dry) for both the water saturation and drying process in laboratory (Guo et al. 2017; Liu et al. 2020). Especially for practical engineering situations such as aquifer discharging, hydraulic fracturing and water-infusion, the water distribution is in a dynamic and non-uniform mode.

To quantitatively or qualitatively investigate the water distribution within the coal/rock samples, non-destructive diagnose techniques including nuclear magnetic resonance (NMR) and neutron radiography (NR) have been used or discussed by scholars. The working principle of NMR is detecting the hydrogen protons (^{1}H) and its energy states of water existing in materials (Zhou et al. 2016). NMR has been successfully used to study the fluid saturation and transport within porous materials including rock and coal (Muir and Balcom 2013; Saito et al. 2002). However, the NMR technique is often limited by hardware constrains, spatial resolution and a lack of inherent fluid-phase sensitivity (Mitchell et al. 2013). Neutron radiography has been explored to provide images of fluid within concrete/rock as thermal neutrons are attenuated to a significant degree by hydrogen, and substances containing hydrogen (De Beer et al. 2004a; Wilding et al. 2005). However, the NR technique is hard to be accessed as neutrons are produced by a beam from a nuclear reactor and thermalized primarily by water and secondary by means of a bismuth crystal that eliminates almost all the primary gamma radiation in the beam (De Beer et al. 2004a). Alternatively, another imaging technique based on X-ray computed tomography with micron scale resolution (μ-CT) has been applied to visualize and measure the internal structural changes of coal due to fluid injection and to understand the influence on the coal porosity and permeability (Nesbitt et al. 2023; Ramandi et al. 2021). Compared with NMR and NR, μ-CT imaging is easy to be accessed and operated. Especially, μ-CT imaging, which is based on variation in density and atomic composition of the scanned objects (Yarmohammadtooski et al. 2017), enables a three-dimensional visualise of the heterogeneous and anisotropic coal samples (Song et al. 2023). Hence, researchers have used μ-CT technique with optimal scanning setting and proper analysis algorithm to capture the rapid moisture change within concrete (Powierza et al. 2019) and timber (Lazarescu et al. 2010) based on the evaluating of the density profile change.

The primary aim of this paper is extending the application of μ-CT imaging to explore the moisture penetration and distribution within hard coal samples during water saturation process as the water infusion method has long been used for burst mitigating of hard coal, while the moisture state after infusion of the coal has been reported by very little literature. The working principle and procedures of μ-CT imaging were firstly introduced. Then, the determination equation of moisture distribution based on density profile was established. A mathematical model of water distribution was put forward for the verification of distribution mode by comparison of failure behaviour between experimental and numerical results. The paper has demonstrated that μ-CT can be used for non-destructively imaging the moisture distribution within coal samples.

2 Image acquisition and reconstruction

2.1 X-ray CT imaging in coal research

X-ray CT, commonly used for tumors and bone fracture recognition by their contrast with surrounding tissue, is based on the two-dimensional radiographic projection of a three-dimensional specimen as the X-ray attenuation correlates with the density of the material (Stelzner et al. 2019). For the scanned images, the digital array reflects the attenuation coefficient values associated with voxel. These values are obtained and scaled by reconstruction algorithm based on the observed attenuation values combined with the Beer Lambert law (Wildenschild et al. 2002).

$$I = I_0 \exp(-\mu x) \tag{1}$$

where I is the attenuated intensity after the X-rays have passed through an object of thickness x, I_0 is the incident radiation intensity, and μ is the linear attenuation coefficient (AC).

With repeated scanning from different viewing angles over a complete 360° rotation, a three-dimensional visualizing of sample structure can be achieved using special reconstruction algorithms. Due to its non-destructive imaging ability, X-ray CT technique has been used to the study of coal including but not limited to observation of swelling/

Table 1 Skyscan1275 X-ray μ-CT Scanner Specification

Parameter	Minimum voxel size (μm)	Maximum scanning diameter(mm)	Maximum scanning height(mm)	Peak voltage(kV)	Maximum resolution(pixels)
Value	4	96	120	100	1944 × 1536

Note The maximum scanning height is achieved by automatically connected partial scans of 50 mm height for a single scan

Table 2 Quality test results of coal

Ash content (%)	Volatile matter(%)	Sulphur(%)	Phosphorus(%)	Fixed carbon(%)	Colloid thickness(mm)
11.23	32.08	0.63	0.015	59.86	<8 PPM

shrinking and fracturing accompanying multi-phase fluid flow (Yarmohammadtooski et al. 2017), determination of porosity and permeability characterization under different thermal/mechanical conditions (Ramandi et al. 2016), evaluation of gas absorption and transport within pore structures (Karacan and Okandan 2001), and imaging the fracture and cleat systems of coal as natural or subject to different loading conditions (Zhao et al. 2021). A comprehensive review on the X-ray CT application in coal study has been made in recent publication (Mathews et al. 2017).

2.2 Image acquisition

The X-ray micro-tomography Skyscan1275, which is a desk-top laboratory scanning system, was used to perform the scanning of coal samples with different saturation time. The whole system includes a μ-CT scanner and a computer with built-in software package for image scanning, reconstructing and further analysing. The μ-CT scanner, with specifications shown in Table 1, basically contains a microfocus X-ray source, a two-dimensional X-ray detector and precision object manipulator. The manipulator can position and rotate the sample under the software control to alter the image magnification by changing the relative position between the sample and X-ray source.

A typical hard coal sourced from Binchang coal field in China was used for the saturation and scanning as this coal seam is under the influence of aquifer. The coal information was listed in Table 2. The coal is classified as hard coal with an average strength above 15 MPa. Besides, hydraulic fracturing is normally used to crack hard coal for enhancing gas permeability or eliminating burst potential. The understanding of water distribution within hard coal is meaningful for providing fundamental knowledge of water influence on the coal properties for these on-site practices. As the coal samples with different saturation time will be uniaxially loaded to compare the failure mode with numerical model, all samples were processed into ISRM standard samples (Yang et al. 2020) with 100 mm height and 50 mm diameter.

The coal sample as natural or with different saturation time is placed in the centre of the scanner's field of view and hold by the manipulator seat teeth. Then the scan settings were optimized in the control software. To enable a full view of the whole sample with 50 mm diameter, the area of each pixel is set as 33 × 33 μm as the sample will be beyond the range of 2-dimentional detector with a smaller pixel size. The scanning energy and image resolution are set to the maximum capacity of the scanner. To construct a detailed visualization of the sample, the sample is scanned for 360º with 0.2º interval for each scan. The whole scan setting and adjusting process is shown in Fig. 1.

For CT scan, the linear attenuation coefficient (AC), which is the parameter that describe the attenuation property, will change with the physical properties of the scanned sample. Moisture, coal matrix and air differ greatly in density and AC value (Du et al. 2019). The μ-CT scanner can record the AC change in 10^{-6} level for each pixel size, which enables the quantitative estimation of moisture change according to AC value for each pixel range.

2.3 Image reconstruction

The reconstruction of all scanned images is needed as the cone X-ray beam produced by point source can only generate one slice of two-dimensional projection for each single scan from a particular angle. The sample rotate 360º with a 0.2º rotation interval for acquiring a shadow image at each angular position. All these projections then used for the construction of the virtual slices through the sample as shown in Fig. 2. The sample can be previewed with particular reconstruction fine-tunning setting including smoothing, misalignment compensation, ring artifacts reduction, rotation beam-hardening correction to generate the cross-section image with clear internal structure and best resolution. The setting can be repeatedly adjusted till the quality of preview cross-section is satisfied. The reconstruction task for each sample can be added into batch or be started reconstruction immediately. Finally, the raw data cross-sections are then generated using the reconstruction algorithm. The images immediately after reconstruction is not ready to be used for further analysis as the density contrast cannot be reflected. With further processing such as background colour change and sample cross-section colour range, the images will clearly show the density change within the sample.

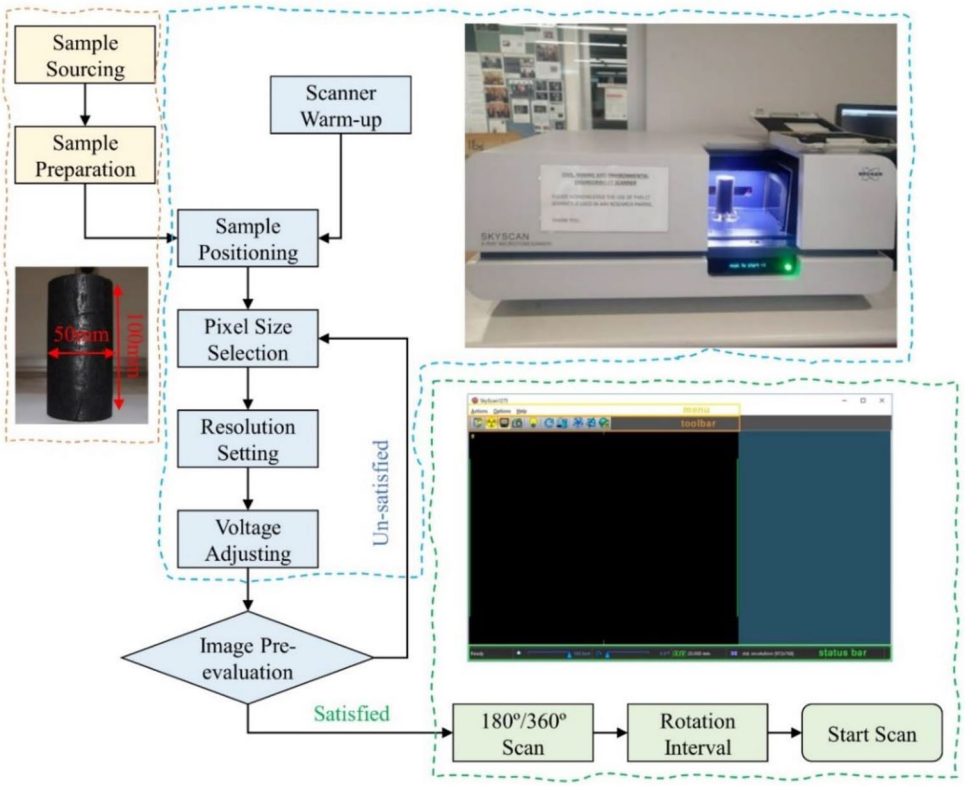

Fig. 1 Flowchart of image acquisition by μ-CT scanner

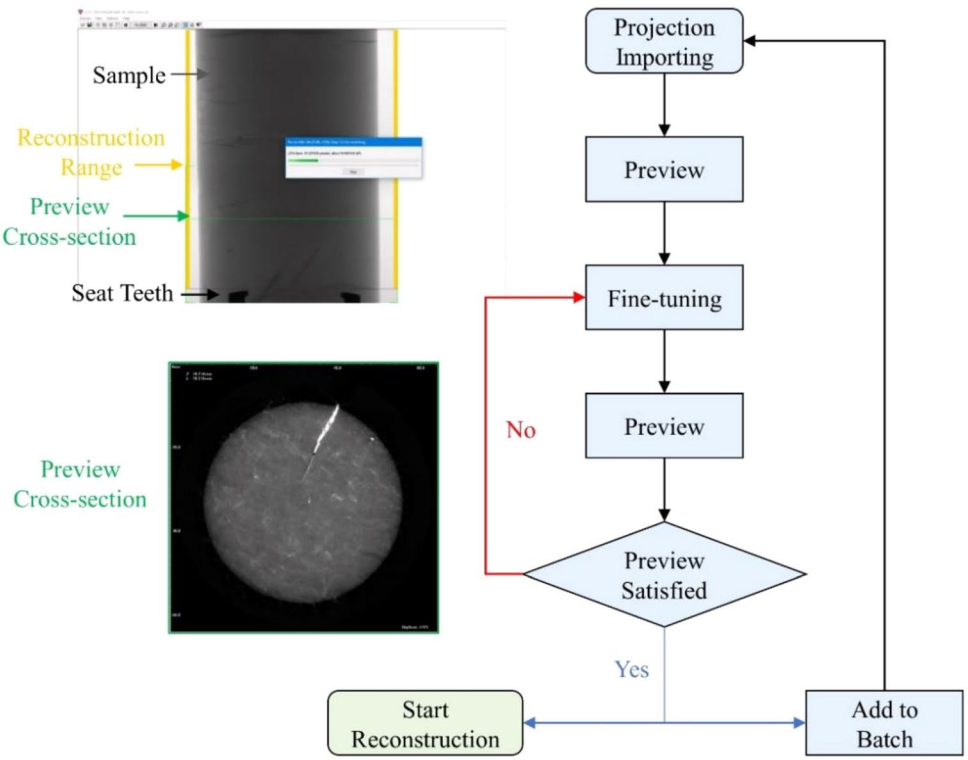

Fig. 2 Flowchart of image construction

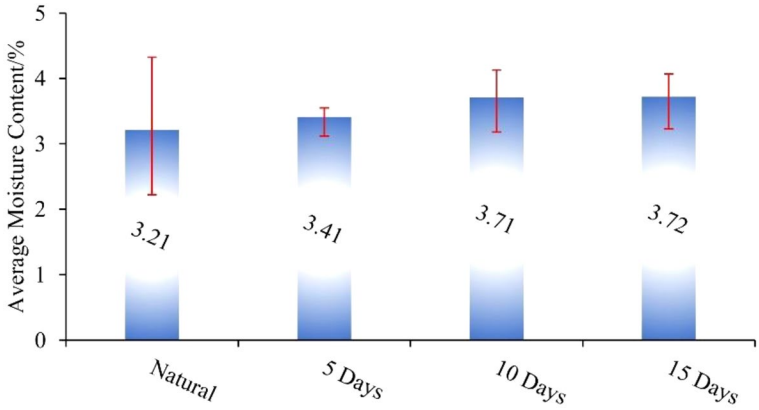

Fig. 3 Moisture content of coal samples with natural state and different infusion time determined by weighting method

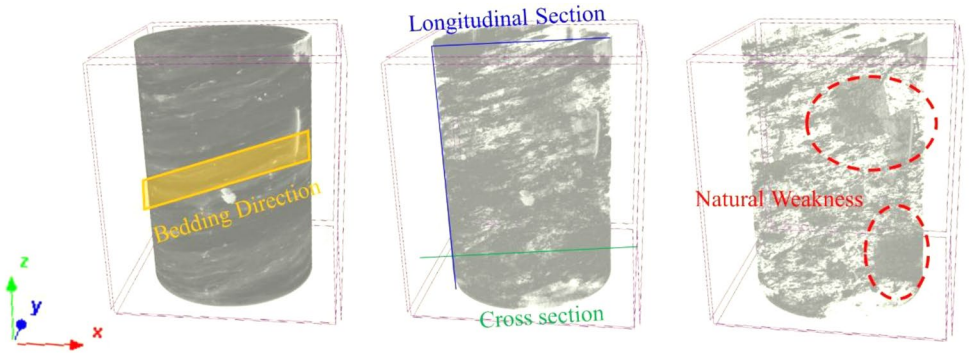

Fig. 4 Reconstructed 3D view of internal structure of coal sample

3 Moisture penetration and distribution

3.1 Qualitative moisture analysis

To determine the natural moisture content and moisture change during infusion process of coal samples, the moisture content of in total 5 samples is determined by oven-drying as shown in Fig. 3. These five samples were in the water for the planned saturation time and then were taken out for weighting and CT scanning. The whole test process included 5 samples to determine the average moisture content to avoid the data variation caused by sample differences. The error bar each group was plotted for each planed saturation stage in Fig. 3. It can be seen that the moisture increase of the hard coal sample is very limited with 15 days of saturation. The moisture content of natural samples has the highest discreteness compared with other groups, which can be reasonably explained by the inhomogeneous properties of coal samples. The moisture content within same group tends to be more equal after water saturation. The average moisture content increased 0.5% at first 10 days saturation but only increased 0.01% at the last 5 days saturation period. However, the clear demonstration of water distribution during infusion process needs to be visualized by cross-sectional image of CT scanning.

As expected, the μ-CT scanning can clearly demonstrate the internal structures such as bedding angle and natural weakness of coal sample as shown in Fig. 4. The sequential images (Fig. 5) of reconstructed scanning (Fig. 4) results exhibited the increase in density within the coal sample.

Basically, the moisture distribution is systematically increase with the distance to the image centre, which can be interpreted as the infusion of the sample is started from the surface area. The obvious change of the AC of coal sample after infusion can be observed compared with the AC profile of natural state sample. The moisture in the core part of the sample is also increasing with the infusion time. But the increasing level is much less than the surface area as suggested by the colour change. Besides, the AC profile of the day 10 and 15 are highly similar, which can also support that the moisture content has very limited increase after day 10 as shown in Fig. 3. The onsite water injection into coal has also indicated the strong water resistance of hard coal samples (Cheng et al. 2012), which is related to its low permeability and undeveloped pore structure. Especially for soft coal with developed pore system, the water penetration process can be obviously observed.

The longitudinal view along the centre of the sample is plotted in Fig. 6. The density change can also be observed at the natural weakness (Area 2) of the sample as the AC has been greatly increased due to moisture increase. Area 2 should storage more moisture as its dark colour range has been decreased after water infusion. The density of coal is 1.38 g/cm^3 and water is 1 g/cm^3, which means the density

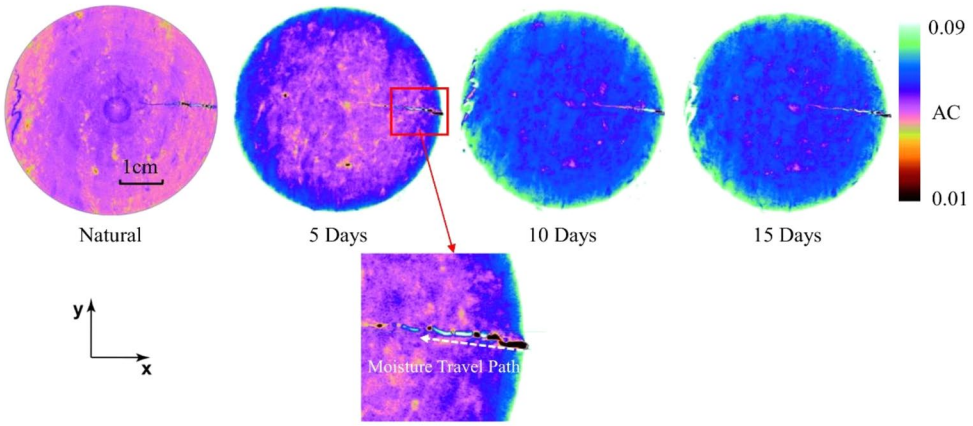

Fig. 5 Cross section view at $Z=22$ mm

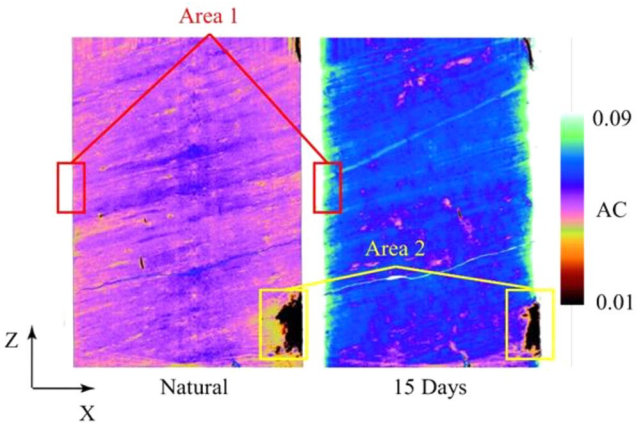

Fig. 6 Longitudinal view at $Y=25$ mm

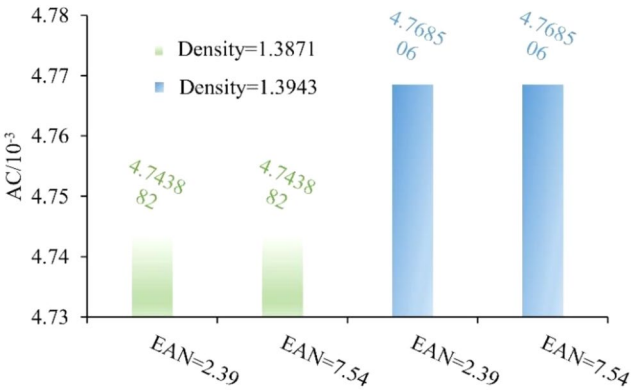

Fig. 7 ACs with different EAN and density

change caused by water sorption (10^{-3} level) can be quantitatively analysed based on the change (10^{-6} level) of AC value (see Fig. 7).

3.2 Quantitative moisture analysis

The basic parameter measured in each pixel of the re-constructed image is the AC, which depends on both electron density (bulk density) and atomic number (Karacan and Okandan 2001):

$$\mu = \rho\left(a + b\frac{Z^{3.8}}{E^{3.2}}\right) \tag{2}$$

where a is the Kline-Nishina coefficient, Z is the effective atomic number (EAN), E is the photon energy in keV and $b = 9.80 \times 10^{-24}$.

On of the most widely used methods for determining the effective atomic number below 150 keV is by:

$$Z = \left(\sum f_i Z_i^{3.8}\right)^{\frac{1}{3.8}} \tag{3}$$

where f_i is the fraction of the total number of electrons contributed by element i, and Z_i is the atomic number of element i. In Eq. (3), f_i is defined as (Karacan 2003):

$$f_i = \frac{\left(\frac{\omega_i}{A_i}\right)Z_i}{\sum_i\left(\frac{\omega_i}{A_i}\right)Z_i} \tag{4}$$

where ω_i is the mass percentage, and A_i is the atomic mass.

As water consists of H_2O, the EAN is regarded as a constant 7.54 (Karacan et al. 2003). The EAN for coal is 2.39 in literature (Ochbelagh et al. 2015). Then the Kline-Nishina coefficient for coal determined according to Eq. (2) based on the average AC of the natural coal is 3.42×10^{-3}. Considering water only accounts for small percentage of the total weight, the EAN of sample will only have very minor change before and after water penetration. However, to be more confident about neglecting the AC change caused by EAN, the ACs are calculated for EAN with either 2.39 and 7.54 as listed in Fig. 3, which also demonstrated that EAN has limited effect on the AC value compared with density.

The density of water infused sample can also be acquired by:

$$\rho = \frac{\rho_{\text{coal}}(1-w_{\text{n}})}{1-w} \tag{5}$$

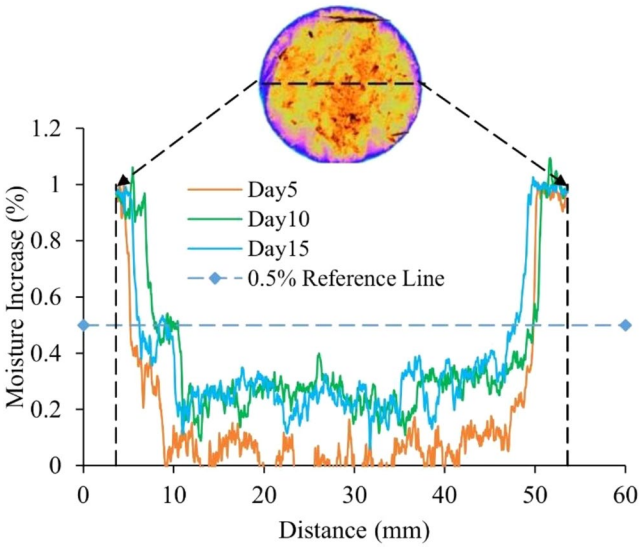

Fig. 8 Change of moisture increase distribution with distance to the centre

where ρ_{coal} is the density of coal with natural moisture content w_n, and w is the moisture content of infused coal.

Thus, the moisture content of water infused coal, or a single pixel can be determined by the AC value:

$$w = 1 - \frac{\mu\rho_{coal}(1-w_n)}{a+b\frac{Z^{3.8}}{E^{3.2}}} \quad (6)$$

Hence, the AC value is transferred to moisture increase based on Eq. (6) as shown in Fig. 8. It can be seen from the figure that only the outside 10 mm area of the sample have more than 0.5% moisture increase during the water penetration process. The internal core of the sample has only about 0.2% moisture increase. However, the outside 10 mm area accounts for 64% of the area of the sample. Hence, the overall moisture increase after infusion of coal sample will be very close to the average moisture increase of outside area, while the internal distribution is significantly non-uniform.

The overall moisture content increase determined by CT-scanning and oven drying are compared in Fig. 9. The determined values are highly consistent with each other as the squared error are below 0.1. However, considering the assumption made during the calculation process based on AC value such as constant EAN, homogeneous property and uniform moisture content on the integral ring (same distance to the centre), the errors related to these factors are counteracted with each other. The influence of these factors on the final results deserves more research in the future to get a more confident equation of quantitative moisture analysis.

4 Conclusions

Observation of the water penetration process and water distribution in the coal matrix will be beneficial for the understanding of the fluid-solid coupling mechanism in gas and coal recovery process. This paper presents a novel visualization method of moisture penetration and distribution within hard coal based on the application of X-ray micro-CT scanning. The equations for quantitively determining the moisture distribution are provided in this paper. The following conclusions can be extracted from the paper:

(1) This non-destructive technique can be applied to precise measurement of water movement during coal sample infusion/drying hence to understand the fluid-coal dynamic process.
(2) As observed by CT images and verified by failure mode, the moisture concentrates on the surface 10 mm area of hard coal, which will cause more damage to the surface area of the sample during loading process.
(3) For outburst and coal burst controlling by water infusion, the natural infusion process only can cause limited influence on the deep area. The moisture increase level have sharp decrease with the increase of distance to the

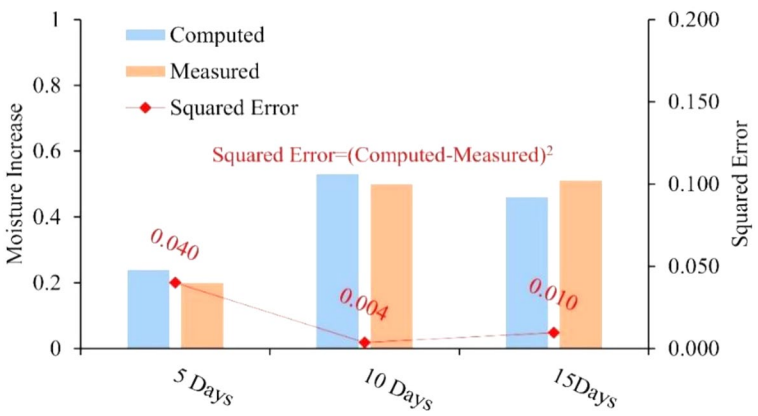

Fig. 9 Moisture increases determined by CT scanning and oven drying

moisture source as observed from the quantitative and qualitative analysis of moisture distribution.

(4) Based on the same principle, the technique may be applied to explore the rock/coal damage caused by gas/steam fracturing, but the effectiveness needs to be further verified as the density of gas/steam is much lower than water.

(5) Giving that mineral dissolution or other factors could induce the AC change as well, this method can be further evaluated with water and coal chemical analysis.

Acknowledgements Not applicable.

Author contributions Lihai Tan: Methodology, Resources, Writing - Original Draft. Ting Ren: Supervision, Writing - Review & Editing. Linming Dou: Supervision, Writing - Review & Editing. Jian Sun: Visualization, Validation. Xiaohan Yang: Formal analysis, Writing - Original Draft. Ming Qiao: Writing - Review & Editing, Conceptualization.

Funding The research is supported by China University of Mining and Technology and University of Wollongong.

Data availability Data are available on request from authors.

Declarations

Competing interests Authors declare no conflict interests.

References

Australian Standard (2005) Method for Testing Rocks for Engineering purposes. Method 1.1 Rock moisture content tests—determination of the moisture content of Rock—Oven Drying Method (Standard Method). Standards Australia, Sydney

Cheng WM, Nie W, Zhou G, Yu YB, Ma YY, Xue J (2012) Research and practice on fluctuation water injection technology at low permeability coal seam. Saf Sci 50(4):851–856

De Beer FC, Middleton MF, Hilson J (2004a) Neutron radiography of porous rocks and iron ore. Appl Radiation Isot 61(4):487–495

Du Y, Sang SX, Pan ZJ, Wang WF, Liu SQ, Fu CQ, Zhao YC, Zhang JY (2019) Experimental study of supercritical CO2-H2O-coal interactions and the effect on coal permeability. Fuel 253:369–382

Guo WY, Tan YL, Yang ZL, Zhao TB, Hu SC (2017) Effect of Saturation Time on the coal Burst liability indexes and its application for Rock Burst Mitigation [journal article]. https://doi.org/10.1007/s10706-017-0300-2. Geotechnical and Geological Engineering

Karacan CÖ (2003) Heterogeneous sorption and swelling in a confined and stressed coal during CO2 injection. Energy Fuels 17(6):1595–1608

Karacan CO, Okandan E (2001) Adsorption and gas transport in coal microstructure: investigation and evaluation by quantitative X-ray CT imaging. Fuel 80(4):509–520

Karacan CÖ, Halleck PM, Grader AS, Mitchell GD (2003) Kinetics of the Physical Changes and Gas Storage Capacity Induced by Carbon Dioxide Sequestration in Coal. Second Annual Conference on Carbon Sequestration Proceedings

Lazarescu C, Watanabe K, Avramidis S (2010) Density and moisture profile evolution during timber drying by CT scanning measurements. Drying Technol 28(4):460–467

Li ZB, Ren T, Black D, Qiao M, Abedin I, Juric J, Wang M (2023a) In-situ gas contents of a multi-section coal seam in Sydney basin for coal and gas outburst management. Int J Coal Sci Technol 10(1):62

Li ZB, Ren T, Li XC, Cheng YP, He XQ, Lin J, Qiao M, Yang XH (2023b) Full-scale pore structure characterization of different rank coals and its impact on gas adsorption capacity: a theoretical model and experimental study. Energy 277:127621

Liu YB, Yin GZ, Li MH, Zhang DM, Huang G, Liu P, Liu C, Zhao HG, Yu BC (2020) Mechanical properties and failure behavior of dry and water-saturated anisotropic coal under true-triaxial loading conditions. Rock Mech Rock Eng 53(11):4799–4818

Liu A, Liu SM, Liu P, Wang K (2021) Water sorption on coal: effects of oxygen-containing function groups and pore structure. Int J Coal Sci Technol 8(5):983–1002

Liu ZY, Wang G, Li JZ, Li HX, Zhao HF, Shi HW, Lan JL (2022) Water-immersion softening mechanism of coal rock mass based on split Hopkinson pressure bar experiment. Int J Coal Sci Technol 9(1):61

Liu XW, Chen HX, Liu B, Wang S, Liu QS, Luo Y, Luo J (2023) Experimental and numerical investigation on failure characteristics and mechanism of coal with different water contents. Int J Coal Sci Technol 10(1):49

Ma D, Duan HY, Zhang JX, Bai HB (2022) A state-of-the-art review on rock seepage mechanism of water inrush disaster in coal mines. Int J Coal Sci Technol 9(1):50

Mathews JP, Campbell QP, Xu H, Halleck P (2017) A review of the application of X-ray computed tomography to the study of coal. Fuel 209:10–24

McCarter MK (2010) Water Infusion For Bump Control; Laboratory Feasibility Tests On Utah Coal. 44th US Rock Mechanics Symposium and 5th US-Canada Rock Mechanics Symposium

Mitchell J, Chandrasekera TC, Holland DJ, Gladden LF, Fordham EJ (2013) Magnetic resonance imaging in laboratory petrophysical core analysis. Phys Rep 526(3):165–225

Muir CE, Balcom BJ (2013) A comparison of magnetic resonance imaging methods for fluid content imaging in porous media. Magn Reson Chem 51(6):321–327

Nesbitt K, Aziz F, Mahoney M, Chalup S, Lamichhane BP (2023) Classifying coke using CT scans and landmark multidimensional scaling. Int J Coal Sci Technol 10(1):7

Ochbelagh DR, Masalla AV, Abadi AY (2015) Estimation of effective atomic numbers of polyethylene and coal using Compton Scattering. University of Engineering and Technology Taxila. Tech J 20(4):50

Pan ZJ, Connell LD, Camilleri M, Connelly L (2010) Effects of matrix moisture on gas diffusion and flow in coal. Fuel 89(11):3207–3217

Perera MSA, Ranjith PG, Peter M (2011) Effects of saturation medium and pressure on strength parameters of Latrobe Valley brown coal: carbon dioxide, water and nitrogen saturations. Energy 36(12):6941–6947

Powierza B, Stelzner L, Oesch T, Gollwitzer C, Weise F, Bruno G (2019) Water migration in one-side heated concrete: 4D in-situ CT monitoring of the moisture-clog-effect. J Nondestr Eval 38(1):1–11

Ramandi HL, Mostaghimi P, Armstrong RT, Saadatfar M, Pinczewski WV (2016) Porosity and permeability characterization of coal: a micro-computed tomography study. Int J Coal Geol 154:57–68

Ramandi HL, Pirzada MA, Saydam S, Arns C, Roshan H (2021) Digital and experimental rock analysis of proppant injection into naturally fractured coal. Fuel 286:119368

Saito K, Hasegawa K-i, Komaki I, Katoh K (2002) In-situ high-temperature magnetic resonance imaging of coals using prepared magnetization SPRITE techniques. Energy Fuels 16(3):575–585

Song SK, Ren T, Dou LM, Sun J, Yang XH, Tan LH (2023) Fracture features of brittle coal under uniaxial and cyclic compression loads. Int J Coal Sci Technol 10(1):9

Stelzner L, Powierza B, Oesch T, Dlugosch R, Weise F (2019) Thermally-induced moisture transport in high-performance concrete studied by X-ray-CT and 1H-NMR. Constr Build Mater 224:600–609

Wildenschild D, Vaz CMP, Rivers ML, Rikard D, Christensen BSB (2002) Using X-ray computed tomography in hydrology: systems, resolutions, and limitations. J Hydrol 267(3–4):285–297

Wilding M, Lesher CE, Shields K (2005) Applications of neutron computed tomography in the geosciences. Nuclear instruments and methods in Physics Research Section A: Accelerators, Spectrometers. Detectors Assoc Equip 542(1):290–295. https://doi.org/10.1016/j.nima.2005.01.151

Yang XH, Ren T, Tan LH (2020) Estimation of average ejection velocity generated by rib burst under compression load. Int J Rock Mech Min Sci 128:104277. https://doi.org/10.1016/j.ijrmms.2020.104277

Yao QL, Chen T, Tang CJ, Sedighi M, Wang SW, Huang QX (2019) Influence of moisture on crack propagation in coal and its failure modes. Eng Geol 258:105156

Yarmohammadtooski Z, Salmachi A, White A, Rajabi M (2017) Fluid flow characteristics of Bandanna coal formation: a case study from the Fairview Field, eastern Australia. Aust J Earth Sci 64(3):319–333

Zhao Y, Konietzky H, Herbst M (2021) Damage evolution of coal with inclusions under Triaxial Compression. Rock mechanics and rock engineering, pp 1–18

Zhou ZL, Cai X, Cao WZ, Li XB, Xiong C (2016) Influence of water content on mechanical properties of rock in both saturation and drying processes. Rock Mech Rock Eng 49(8):3009–3025